ORIGINAL ARTICLE

Teleocidin A2 inhibits human proteinase-activated receptor 2 signaling in tumor cells

Sonja Stahn[1], Lisa Thelen[1], Ina-Maria Albrecht[1], Jens Bitzer[2], Thomas Henkel[2] & Nicole Elisabeth Teusch[1]

[1]Bio-Pharmaceutical Chemistry, Faculty of Applied Natural Sciences, Cologne University of Applied Sciences, ChemPark Leverkusen, Leverkusen, Germany
[2]IMD Natural Solutions GmbH, Dortmund, Germany

Abstract

Enhanced expression of the proteinase-activated receptor 2 (PAR2) is linked to cell proliferation and migration in many cancer cell types. The role of PAR2 in cancer progression strongly illustrates the need for PAR2-inhibiting compounds. However, to date, potent and selective PAR2 antagonists have not been reported. The natural product teleocidin A2 was characterized against PAR2-activating peptide SLIGKV-NH$_2$, and trypsin-induced PAR2-dependent intracellular Ca^{2+} mobilization in tumor and in primary endothelial or epithelial cells. Further biochemical and cell-based studies were conducted to evaluate teleocidin specificity. The antagonizing effect of teleocidin A2 was confirmed in PAR2-dependent cell migration and rearrangement of actin cytoskeleton of human breast adenocarcinoma cell line (MDA-MB 231) breast cancer cells. Teleocidin A2 antagonizes PAR2-dependent intracellular Ca^{2+} mobilization induced by either SLIGKV-NH$_2$ or trypsin with IC$_{50}$ values from 15 to 25 nmol/L in MDA-MB 231, lung carcinoma cell line, and human umbilical vein endothelial cell. Half maximal inhibition of either PAR1 or P2Y receptor-dependent Ca^{2+} release is only achieved with 10- to 20-fold higher concentrations of teleocidin A2. In low nanomolar concentrations, teleocidin A2 reverses both SLIGKV-NH$_2$ and trypsin-mediated PAR2-dependent migration of MDA-MB 231 cells, and has no effect itself on cell migration and no effect on cell viability. Teleocidin A2 further controls PAR2-induced actin cytoskeleton rearrangement of MDA-MB 231 cells. Thus, for the first time, the small molecule natural product teleocidin A2 exhibiting PAR2 antagonism in the low nanomolar range with potent antimigratory activity is described.

Abbreviations

A549, lung carcinoma cell line; ANOVA, analysis of variance; ATP, adenosine 5′ triphosphate; DMEM, Dulbecco's modified Eagle's medium; ERK1/2, signal-regulated kinase 1/2; FCS, fetal calf serum; GPCR, G protein-coupled receptor; HMEC, human mammary epithelial cells; HRP, horseradish peroxidase; HUVEC, human umbilical vein endothelial cells; MAPK, mitogen-activated protein kinase; MDA-MB 231, human breast adenocarcinoma cell line; mPASMC, murine pulmonary artery smooth muscle cells; NSCLC, non–small cell lung cancer; PAR1, proteinase-activated receptor 1; PAR2, proteinase-activated receptor 2; PASMC, pulmonary artery smooth muscle cells; PKC, protein kinase C; PMA, phorbol 12-myristate 13-acetate; PyMt, polyoma middle T; Rac1, ras-related C3 botulinum toxin substrate 1; RhoA, ras homolog family member A; ROCK1/2, rho-associated, coiled-coil containing protein kinase 1/2; TF, tissue factor; WT, wild type.

Introduction

Proteinase-activated receptors (PARs) are the members of the seven transmembrane G protein-coupled receptor (GPCR) superfamily. To date, four PARs (PAR 1–4; cloned and named in order of their discovery) have been described (Vu et al. 1991; Nystedt et al. 1994; Ishihara et al. 1997; Xu et al. 1998). PARs share a unique mechanism of receptor activation by proteolytic cleavage of the extracellular N-terminal domain by tryptic serine proteinases. In contrast to thrombin-regulated PAR1, 3, and 4, proteinase-activated receptor 2 (PAR2) can be specifically activated by trypsin-like proteases, including trypsin, tryptase, and coagulation proteases upstream of thrombin, complexes of tissue factor (TF) with FVIIa or FXa, respectively (Nystedt et al. 1994; Rothmeier and Ruf 2012). Short synthetic PAR2 peptide sequences representing the first six amino acids of the cleaved N-terminus can directly activate the receptor (Scarborough et al. 1992).

Upon activation, PAR2 couples to heterotrimeric G proteins $G_{q/11}$, G_i, and $G_{12/13}$ and additionally recruits β-arrestins subsequently initiating receptor internalization and degradation. Moreover, β-arrestins have been reported to induce G protein-independent signaling and regulation of cell migration (DeFea et al. 2000; Zoudilova et al. 2010). Despite the described role of PAR2 in the migration of various cell types (Rothmeier and Ruf 2012), the respective underlying signaling cascade still remains elusive, presumably based on cell-type specificity. For instance, Zhu et al. (2011) demonstrated a PAR2-ras homolog family member A (RhoA)-dependent migration of endothelial cells, whereas in colon cancer a pathway encompassing c-jun/AP-1 activation and upstream protein kinase C (PKC)α and ERK1/2 activation contributed to cell migration (Hu et al. 2013). In general, small Rho GTPases are important regulators of a dynamic actin cytoskeleton in migratory cells (Raftopoulou and Hall 2004). In line, rhoA activation was demonstrated downstream to PAR2 inducing the formation of stress fibers and focal adhesions (Greenberg et al. 2003; Sriwai et al. 2013; Suen et al. 2014). Furthermore, Su et al. (2009) described PAR2-induced activation of a c-src – ras-related C3 botulinum toxin substrate 1 (Rac1) – JNK 1/2 signaling axis leading to paxillin phosphorylation finally resulting in increased cell motility of breast cancer cells.

Beside a role in regulating various physiological functions ranging from vasoregulation to inflammation and nociception (reviewed in Rothmeier and Ruf 2012; Gieseler et al. 2013; Bao et al. 2014), there is growing evidence for a function of PAR2 in cancer progression (Elste and Petersen 2010). In this context, various in vitro studies including breast (Hjortoe et al. 2004; Su et al. 2009), colon (Hu et al. 2013), pancreatic (Shi et al. 2013; Xie

et al. 2015), lung adenocarcinoma (Huang et al. 2013), and hepatocellular carcinoma (Nakanuma et al. 2010; Kaufmann et al. 2011) cells revealed a role of PAR2 signaling in cancer cell proliferation as well as in migration and invasion, presumably linked to increased metastatic potential. In an in vivo study of spontaneous development of mammary adenocarcinoma in polyoma middle T (PyMt) mice, PAR2, in contrast to PAR1, promoted the transition to invasive carcinoma (Versteeg et al. 2008). Furthermore, from a clinical perspective, elevated PAR2 expression in isolated tumor tissue could be associated with increased malignancy grades in breast and high-grade astrocytoma tumors, lung carcinoma, and gastric and esophageal cancer (D'Andrea et al. 2001; Rydén et al. 2010; Svensson et al. 2011; Li et al. 2014). Moreover, in patients suffering from breast cancer, elevated levels of PAR2 were linked to a bad prognosis (Rydén et al. 2010).

Lessons from studies using receptor-activating peptides and genetically receptor-deficient mice have predominantly contributed to elucidation of functions of PARs. However, the distinct role of PAR2 in multiple pathophysiological contexts illustrates the need for PAR2 targeting and inhibiting compounds to further investigate and understand PAR2 signaling. Primarily, the described tumor-promoting effects of PAR2 provide the basis for the development of a receptor antagonist as a novel therapeutic strategy in cancer treatment. To date, all PAR2 antagonists described are limited in potency, namely ENMD-1068 (IC_{50} 2.5–5 mmol/L; Kelso et al. 2006), K14585 (IC_{50} 5–10 μmol/L; Goh et al. 2009; Kanke et al. 2009), GB88 (IC_{50} 2 μmol/L; Suen et al. 2012), and C391 (IC_{50} 1,3 μmol/L; Boitano et al. 2015).

Here, we present for the first time the natural product teleocidin A2 (Fig. 1) as a potent inhibitor of PAR2 signaling. In previous decades, teleocidins were mainly categorized as tumor promotors via a PKC-activating mechanism, however, in concentrations ranging from 100 nmol/L up to 10 μmol/L (Fujiki et al. 1984; Arcoleo and Weinstein 1985; Imamoto et al. 1993). In this study, teleocidin A2 specifically inhibits PAR2-induced Ca^{2+} release in the investigated tumor cell lines human breast adenocarcinoma cell line (MDA-MB 231), lung carcinoma cell line (A549), as well as in human umbilical vein endothelial cells (HUVEC) at low nanomolar concentrations (15–25 nmol/L). Teleocidin A2 suppresses PAR2-induced Ca^{2+} mobilization rather than inhibiting Ca^{2+} mobilization initiated by other endogenously expressed G_q-coupled GPCRs. Finally, our studies reveal teleocidin A2 to be able to inhibit PAR2-induced, Rac1-dependent cell migration by controlling PAR2-initiated actin cytoskeletal changes.
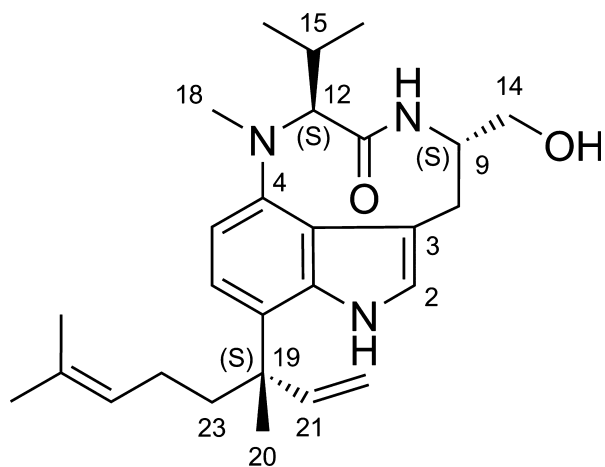
Figure 1. Chemical structure of teleocidin A2.

Materials and Methods

Cell culture

To explore PAR2 signaling and to study the effect of teleocidin A2 on endogenous receptors, human breast adenocarcinoma MDA-MB 231, lung carcinoma A549, HUVEC, noncancerous human mammary epithelial cells (HMEC), and murine pulmonary artery smooth muscle cells isolated from pulmonary arteries of wild-type and PAR2-deficient mice (mPASMC WT, mPASMC PAR2$^{-/-}$) (ten Freyhaus et al. 2015) were used. MDA-MB 231 cells were obtained from European Collection of Cell cultures (Salisbury, U.K.) and grown in Leibovitz's L15 containing 15% fetal calf serum (FCS) and 2 mmol/L glutamine. A549 cells were purchased from German Collection of Microorganisms and Cell Cultures (Braunschweig, Germany) and cultured in Dulbecco's modified Eagle's medium (DMEM) along with 10% FCS. Murine PASMC WT and PAR2$^{-/-}$ were a kind gift from Prof. Dr. Rosenkranz (University Hospital Cologne). They were cultured in DMEM, 20% FCS. Media was supplemented with 100 units mL^{-1} penicillin and 100 μg mL^{-1} streptomycin. HUVECs and HMECs were cultured as indicated by Lonza (Basel, Switzerland). Cells were incubated in humidified atmosphere at 37°C containing 5% CO_2 or in case of MDA-MB 231 in the absence of CO_2. For cell dissociation during passaging, trypsin-free cell dissociation buffer was applied.

Intracellular calcium mobilization

Kinetic measurements of intracellular calcium mobilization were performed as previously described by Suen et al. (2012) using Fluo-8 (4 μmol/L) as indicator dye. To examine inhibitory effects of PAR2 compounds, cells were incubated for 10 min with different compound concentrations

before agonist stimulation. Stimulation with the agonists SLIGKV-NH$_2$, SLIGRL-NH$_2$, trypsin, TFLLR-NH$_2$, thrombin, and adenosine 5′ triphosphate (ATP) was performed with the injector unit from Tecan Infinite M1000 Pro microplate reader Tecan (Maennedorf, Switzerland) after 16 sec of baseline measurement. Fluorescence was measured using excitation at $\lambda = 490$ nm and emission at $\lambda = 525$ nm. The maximum fluorescence signal was generated with the calcium ionophore A23187; H_2O served as a control for background fluorescence.

Cell migration assay

PAR2-mediated cell migration was measured using Oris™ Cell Migration Assay (Platypus Technologies, Madison, USA) according to Gough et al. (2011). MDA-MB 231 cells were grown to 80% confluency and seeded overnight at 1.5×10^4 cells per well. Compounds were added as indicated in the results and the cells incubated for 48 h to allow migration. Cells were fluorescently labeled with Track It™ Green purchased from AAT Bioquest (Sunnyvale, CA). Images of single wells were taken using fluorescent microscope Zeiss AxioVert A1 (Zeiss, Jena, Germany) and AxioCam MRm, and migration into detection zones was evaluated by particle analysis in ImageJ (Rasband, W.S., ImageJ, U.S. National Institutes of Health, Bethesda, MD; http://imagej.nih.gov/ij/, 1997–2014).

Cell viability assay

MDA-MB 231 cells were cultivated to 80% confluency and seeded overnight at 1.5×10^4 cells per well into white 96-well clear bottom plates. Compounds were added as indicated in results and in parallel to the cell migration assay and the cells incubated 48 h at 37°C to assess a possible cytotoxic or proliferative effect of different compounds tested in the migration assay. Staurosporin, Dimethyl sulfoxide (DMSO), and cell-free medium were applied as controls. The amount of viable cells was quantified using CellTiter-Glo® Luminescent Cell Viability Assay purchased from Promega (Madison, WI).

Immunofluorescent microscopy

MDA-MB 231 cells were grown to 80% confluency and seeded overnight at 7×10^3 cells per well into black 96-well clear bottom plates. Cells were stimulated with different compounds at defined time points as indicated in results. Fixed and permeabilized cells were stained with 100 nmol/L Alexa Fluor 546-conjugated phalloidin in Phosphate buffered saline (PBS) for 20 min and cell nuclei were visualized with 3 μmol/L a fluorescent DNA

dye, 4',6-diamino-2-phenyl-indol (DAPI) dilactate. Images were taken using fluorescent microscope Zeiss AxioVert A1 and AxioCam MRm, and show representative data from at least three independent experiments.

Radioligand binding assay

Teleocidin A2 binding was tested in a PAR2 (agonist radioligand) binding assay which was mandated to CEREP (ref. no. 2424, Celle l'Evescault, France) as described by Kanke et al. (2005). A competition assay was performed testing teleocidin A2 ($0.5 \, \mu$mol/L, $5 \, \mu$mol/L) versus radiolabeled PAR2 peptide [^{3}H]2-f-LIGRL-NH$_2$ using human PAR2 from recombinant Hela cells. Binding of the radiolabeled peptide was detected after incubation at room temperature for 7 h by scintillation counting. Results showing an inhibition of radiolabeled PAR2 peptide binding higher than 50% indicate at significant binding of test compounds.

Biochemical PKC activation assay

Measurement of PKC activation by teleocidin A2 was based on biochemical PKC and ADP-Glo™ kinase assay (Promega). PKC was incubated with phorbol 12-myristate 13-acetate (PMA) and teleocidin A2 in the presence of phosphatidylserine, ATP, and the PKC substrate neurogranin. Incubation was performed in the absence of diacylglycerol and calcium. After 60-min reaction, the amount of generated ATP was quantified using ADP-Glo™ reagent and kinase detection reagent via luminescence using a Tecan Infinite M1000 Pro microplate reader.

Intracellular PKC activation

The PathScan® phospho-MARCKS (Ser152/156) sandwich ELISA (Cell Signaling Technology, Danvers, MA) was used to measure the level of cellular PKC activation in MDA-MB 231 cells according to the manufacturer's information. Cells were seeded overnight at 1.8×10^6 cells in FCS-free Leibovitz's L15 culture medium to 10 cm dishes (Greiner Bio-One, Kremsmünster, Austria) and treated with $10 \, \mu$mol/L PMA for control, 25 μmol/L SLIGKV-NH$_2$, 25 nmol/L teleocidin A2, or both. Cell lysates of controls and compound-treated cells were generated using lysis buffer supplemented with phenylmethanesulfonyl fluoride. Lysate protein concentrations were determined with Bradford protein assay. Phosphorylated myristolated alanine-rich protein kinase C substrate (MARCKS) protein was detected colorimetrically by biotinylated phospho-MARCKS antibody, horseradish peroxidase (HRP)-coupled streptavidin, and HRP substrate tetramethylbenzidine using Tecan Infinite M200 Pro microplate reader.

Materials

Cell culture media and reagents were purchased from Life Technologies (Carlsbad, CA) or Lonza (Basel, Switzerland). Fetal calf serum was obtained from Biochrom (Berlin, Germany), and Quest Fluo-8™ AM and probenecid from AAT Bioquest. SLIGKV-NH$_2$ was ordered from Bachem (Bubendorf, Switzerland). SLIGRL-NH$_2$, TFLLR-NH$_2$, trypsin, thrombin, ATP, and A23187, as well as EHop-016, Gö6983, Y-27632, PMA, and phosphatidylserine were purchased from Sigma-Aldrich (St. Louis, MO). Cell staining reagents were purchased from Life Technologies. Plates (96 and 384 well) were obtained from Greiner Bio-One. Teleocidin A2, a small molecule originally isolated from *Streptomyces* species, was a kind gift from IMD Natural Solutions, Dortmund, Germany. PAR1 inhibitor vorapaxar was purchased from Axon Medchem (Groningen, the Netherlands).

Group sizes

All data were obtained from a minimum of nine biological replicates of at least three independent experiments. The exact group size for each experiment and the number of independent experiments is provided in the respective figure legend of each dataset. All data subjected to statistical analysis had equal group sizes and were performed with a minimum of nine biological replicates of at least three independent experiments.

Randomization

All cell-based assay samples were completely randomized to control and treatment.

Normalization

Data obtained for parametric statistical analysis were not normalized so all control group values became 1. For calculation of EC$_{50}$ (agonist–response) and IC$_{50}$ (antagonist–response) values, the logarithmic concentration of the agonist or antagonist was plotted against maximum fluorescence change in % of the experiment internal agonist-induced Ca^{2+} release. In Ca^{2+} mobilization studies, data were either normalized to the value of the experiment internal agonist or to the A23187-induced maximum Ca^{2+} release. Normalization had no effect to the overall result of the experiment.

In phospho-MARCKS (Ser152/156) ELISA, the level of MARCKS phosphorylation in untreated cells was taken as the experiment internal control and set to 1.

Data obtained from cell migration studies were normalized against each internal 48-h basal migration control.

Normalization had no effect on the overall outcome of the experiment.

Statistical comparison

Statistical data analysis was performed with equal sample values of a minimum of nine biological values using one-way analysis of variance (ANOVA) followed by Dunnett's post hoc test in case groups were compared with a control or followed by Tukey's post hoc test in case all groups were compared with each other. $P < 0.05$ was used to announce statistically significant difference.

Data analysis

All data were obtained from a minimum of nine biological replicates of three independent experiments and expressed as mean ± SEM. Concentration–response curves were established using nonlinear regression. For calculation of EC_{50} (agonist–response) and IC_{50} (antagonist–response) values, the logarithmic concentration of the agonist or antagonist was plotted against maximum fluorescence change in % of the agonist-induced Ca^{2+} release. Statistical data analysis was performed with equal sample values using one-way ANOVA followed by Dunnett's post hoc test in case groups were compared with a control or followed by Tukey's post hoc test in case all groups were compared with each other. $P < 0.05$ was used to announce statistically significant difference. Curve fitting and data analysis using ANOVA were performed in GraphPad Prism v. 5.04 (GraphPad Software, San Diego, CA).

Ethics

There is currently no clinical relevance of the study. No human subjects were involved in this study.

Results

Teleocidin A2 antagonizes efficaciously PAR2-induced Ca^{2+} mobilization

Intracellular Ca^{2+} mobilization induced by the PAR2-activating protease trypsin or the receptor-specific tethered ligand SLIGKV-NH$_2$ was examined in human cell lines and primary cells. Invasive triple negative breast cancer cell line MDA-MB 231 has been characterized by enhanced PAR2 expression and PAR2-linked increased cell migration (Su et al. 2009). In A549 non–small cell lung cancer (NSCLC) cells, PAR2 has been shown to prevent apoptosis (Huang et al. 2013). Moreover, HUVEC showed PAR2 upregulation and activation under hypoxic

conditions resulting in release of proangiogenic factors (Svensson et al. 2011).

EC_{50} values of SLIGKV-NH$_2$ (EC_{50} 109 ± 9 μmol/L, 23.2 ± 0.8 μmol/L, and 7.46 ± 0.88 μmol/L for HUVEC, A549, and MDA-MB 231, respectively) or trypsin (EC_{50} 112 ± 15 nmol/L, 43.1 ± 8.3 nmol/L, and 4.49 ± 0.41 nmol/L for HUVEC, A549, and MDA-MB 231, respectively) slightly varied between different cell lines, presumably hinting at distinct receptor expression (Fig. 2A–C; Table 1). A constant potency shift to 500- to 1500-fold higher potency of endogenous PAR2 receptor protease trypsin in comparison to SLIGKV-NH$_2$ to trigger Ca^{2+} release was observed. In contrast, in noncancerous mammary epithelial cells (HMEC) no significant calcium mobilization was detected upon stimulation with SLIGKV-NH$_2$ up to a concentration of 10 μmol/L or with trypsin up to 10 nmol/L (Fig. 2D). These findings are consistent with data from qPCR analysis revealing significant upregulated PAR2 expression levels in MDA-MB 231 cells in comparison to HMEC (Table S1).

A library of preselected natural products was subjected to a cell-based screening aiming at identifying novel antagonists of PAR2. Interestingly, this screen previously revealed the natural product teleocidin A2 as a putative PAR2 inhibitor. To confirm its capacity of antagonizing PAR2-induced intracellular Ca^{2+} mobilization, teleocidin A2 was evaluated against two structurally different PAR2 agonists (SLIGKV-NH$_2$ and trypsin).

Teleocidin A2 itself had no significant effect on Ca^{2+} release in MDA-MB 231 and in healthy epithelial breast cells (HMEC) up to 1 μmol/L, suggesting a lack of intrinsic agonistic properties (Fig. 2C and D).

Importantly, in contrast to all PAR2 inhibitors reported to date, teleocidin A2 blocked PAR2-induced Ca^{2+} signaling with efficacy in the low nanomolar range (IC_{50} 14.0 ± 4.1 nmol/L, 25.8 ± 1.7 nmol/L, 18.1 ± 1.7 nmol/L for HUVEC, A549, and MDA-MB 231, respectively) with SLIGKV-NH$_2$ applied at its respective cell-specific EC_{50} values (Fig. 3A–D, Table 1). It is noteworthy that independent of the cell type, teleocidin A2 displayed similar potency by blocking PAR2-dependent Ca^{2+} release. The amount of teleocidin A2-induced Ca^{2+} inhibition remained stable during the investigated time period of maximal 75 min (Fig. 3E). To further explore the mechanism of teleocidin A2 antagonism, varying concentrations of teleocidin A2 were tested against increasing concentrations of the PAR2 agonist peptide SLIGKV-NH$_2$. Increasing concentrations of teleocidin A2 reduced the maximum response of SLIGKV-NH$_2$-induced intracellular Ca^{2+} mobilization. In the presence of teleocidin, full receptor activation by SLIGKV-NH$_2$ could not be achieved at the highest concentrations applied of the agonist (up to 333 μmol/L; Fig. 3F).
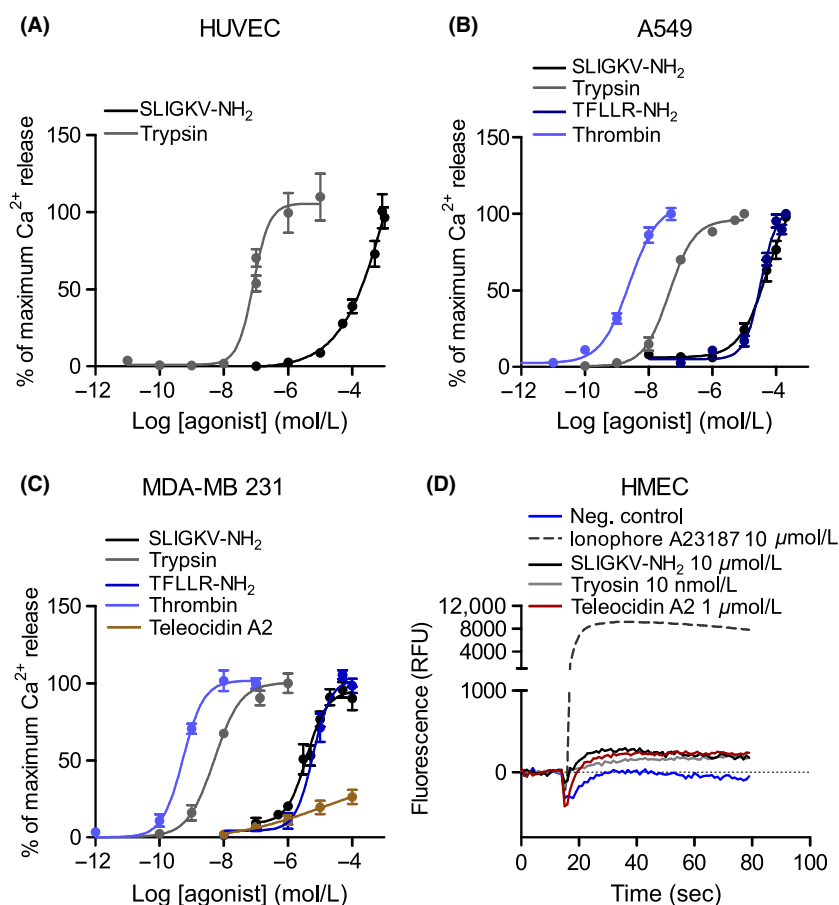
Figure 2. Intracellular Ca^{2+} mobilization in human primary and tumor cells. (A) Concentration-dependent release of intracellular Ca^{2+} by PAR2 agonists SLIGKV-NH_2 and trypsin in HUVEC. (B) Concentration-dependent release of intracellular Ca^{2+} by PAR2 agonists SLIGKV-NH_2 and trypsin and PAR1 agonists TFLLR-NH_2 and thrombin in A549 cells. (C) Concentration-dependent release of intracellular Ca^{2+} by PAR2 agonists SLIGKV-NH_2 and trypsin, PAR1 agonists TFLLR-NH_2 and thrombin, and teleocidin A2 in MDA-MB 231 cells. (D) Kinetics of intracellular Ca^{2+} release in HMEC upon stimulation with 10 μmol/L SLIGKV-NH_2, 10 nmol/L trypsin and 1 μmol/L teleocidin A2. Maximum fluorescence was detected by 10 μmol/L of the ionophore A23187. Results represent data (mean $\pm$ SEM) from at least three independent experiments performed in triplicates. PAR2, proteinase-activated receptor 2; A549, lung carcinoma cell line; MDA-MB 231, human breast adenocarcinoma cell line; HUVEC, human umbilical vein endothelial cell; HMEC, human mammary epithelial cells.

To start assessing selectivity of teleocidin for PAR2, the ability to inhibit Ca^{2+} signaling was observed for the endogenously expressed G_q-coupled GPCRs P2Y and PAR1. PAR1-activating peptide TFLLR-NH_2 and thrombin stimulated PAR1-related intracellular Ca^{2+} release (Fig. 3B and C, Table 1). Teleocidin A2 was tested in the presence of TFLLR-NH_2 at its respective EC_{50} to determine IC_{50} values for PAR1 inhibition. Although teleocidin markedly reduced intracellular Ca^{2+} mobilization initiated by PAR1 in A549 (IC_{50} 200 $\pm$ 38 nmol/L) and MDA-MB 231 cells (IC_{50} 371 $\pm$ 58 nmol/L), it is noteworthy that the compound inhibited PAR1 signaling with a 20-fold potency loss compared to PAR2 (Fig. 3B and C). Furthermore, differences in potency of teleocidin A2-induced blockade of P2Y-initiated Ca^{2+} mobilization could be confirmed. Teleocidin inhibited ATP-induced,

P2Y-dependent Ca^{2+} mobilization with an IC_{50} of 179 $\pm$ 37 nmol/L (Fig. 3C, Table 1).

In contrast to PAR1-activating peptide TFLLR-NH_2, the comparison of inhibition of trypsin- versus thrombin-induced Ca^{2+} release by teleocidin revealed inhibitory effects with IC_{50} values of 54.6 $\pm$ 10.4 nmol/L for trypsin- and of 116 $\pm$ 30 nmol/L for thrombin-induced Ca^{2+} signaling, respectively (Fig. 3D, Table 1). Thus, although less pronounced than for the respective activating peptides, differences in potency of teleocidin A2-induced blockade of PAR2-initiated Ca^{2+} mobilization compared to PAR1-induced Ca^{2+} release by thrombin could be confirmed. The discrepancy in inhibition of thrombin versus TFLLR-NH_2 by teleocidin is consistent with the previously reported unselectivity of thrombin. The generated tethered ligand of PAR1 by thrombin can bind and

Table 1. Summary of EC_{50} values of tested functional agonists and IC_{50} values of teleocidin A2 inhibiting intracellular Ca^{2+} release in the presence of respective agonists.

Receptor	Agonist	Cell line	EC_{50} agonist	IC_{50} teleocidin A2
PAR2	SLIGKV-NH$_2$	MDA-MB 231	$7.46 \pm 0.88\ \mu$mol/L	18.1 ± 1.7 nmol/L
		HUVEC	$109 \pm 9\ \mu$mol/L	14.0 ± 4.1 nmol/L
		A549	$23.2 \pm 0.8\ \mu$mol/L	25.8 ± 1.7 nmol/L
		HMEC	$>500\ \mu$mol/L	n.d.
	Trypsin	MDA-MB 231	4.49 ± 0.41 nmol/L	54.6 ± 10.4 nmol/L
		HUVEC	112 ± 15 nmol/L	n.d.
		A549	43.1 ± 8.3 nmol/L	n.d.
		HMEC	>250 nmol/L	n.d.
PAR1	TFLLR-NH$_2$	MDA-MB 231	$7.15 \pm 0.60\ \mu$mol/L	371 ± 58 nmol/L
		A549	$52.1 \pm 5.0\ \mu$mol/L	200 ± 38 nmol/L
		mPASMC WT	$2.11 \pm 0.46\ \mu$mol/L	24.6 ± 4.2 nmol/L
		mPASMC PAR2$^{-/-}$	$3.09 \pm 0.39\ \mu$mol/L	862 ± 214 nmol/L
	Thrombin	MDA-MB 231	0.53 ± 0.12 nmol/L	116 ± 30 nmol/L
		A549	2.57 ± 0.12 nmol/L	n.d.
		mPASMC WT	0.732 ± 0.086 nmol/L	n.d.
		mPASMC PAR2$^{-/-}$	3.92 ± 0.89 nmol/L	n.d.
P2Y	ATP	MDA-MB 231	254 ± 9 nmol/L	179 ± 37 nmol/L

Data represent mean $\pm$ SEM from three or more independent experiments in triplicates. PAR2, proteinase-activated receptor 2; MDA-MB 231, human breast adenocarcinoma cell line; HUVEC, human umbilical vein endothelial cells; A549, lung carcinoma cell line; HMEC, human mammary epithelial cells; n.d., not determined; mPASMC, murine pulmonary artery smooth muscle cells; WT, wild type; ATP, adenosine 5′ triphosphate.

activate PAR2, resulting in intermolecular PAR2 signaling (Ossovskaya and Bunnett 2004). In contrast, vorapaxar, an FDA-approved PAR1 receptor antagonist (Chackalamannil et al. 2008), failed to inhibit trypsin-induced Ca^{2+} release confirming drug specificity for PAR1 and protease specificity for PAR2 (Fig. S3).

In contrast to teleocidin, PMA inhibits PAR1 and PAR2 comparably

To further evaluate compound selectivity, teleocidin A2 was examined in a biochemical PKC kinase assay. The alkaloid markedly activated purified PKC isoform mix up to 1.3-fold compared to DMSO control in the absence of diacylglycerol and calcium. The level of induced PKC activity was comparable to the tumor-promoting agent PMA (applied at 100 μmol/L) serving as a positive control. In contrast to the efficacious blockade of PAR2-induced intracellular Ca^{2+} mobilization in the biochemical kinase assay, activation of purified PKC by teleocidin A2 could only be shown at high micromolar concentrations (1–100 μmol/L) (Fig. 4A). In the presence of increasing concentrations of PKC inhibitor Gö6983 applied in the intracellular Ca^{2+} mobilization assay, the inhibitory effect of teleocidin A2 on intracellular PAR2 Ca^{2+} release was suppressed in a concentration-dependent manner and finally abolished with 100 nmol/L Gö6983 (Fig. 4B). PKC inhibitor Gö6983 itself, however, had no significant effect on SLIGKV-NH$_2$-induced intracellular Ca^{2+} mobilization.

To explore cellular stimulation of PKC, phosphorylation of the specific endogenous PKC substrate MARCKS at its serine residues 152 and 156 was determined (Heemskerk et al. 1993). As expected, the positive control PMA (10 nmol/L) induced a strong phosphorylation up to threefold, representing a significant PKC activation. SLIGKV-NH$_2$ itself initiated MARCKS phosphorylation up to twofold in comparison to untreated control cells (Fig. 4C). Furthermore, MARCKs was phosphorylated up to 2.7-fold compared to the untreated control in the presence of 25 nmol/L teleocidin A2. In case teleocidin was incubated along with SLIGKV-NH$_2$, the level of MARCKS phosphorylation was comparable to the level induced by teleocidin alone (Fig. 4C).

As PMA has demonstrated in numerous studies to be a strong PKC activator, the inhibitory potential of PMA on PAR2 and PAR1 agonist peptide-induced intracellular Ca^{2+} mobilization was evaluated, respectively. Importantly, PMA inhibited both SLIGKV-NH$_2$- and TFLLR-NH$_2$-mediated Ca^{2+} releases similarly in the low nanomolar range (IC_{50} 5.89 ± 2.78 and 7.47 ± 3.18 nmol/L) (Fig. 4D). Thus, in contrast to the described pronounced PAR2 blocking effect for teleocidin, PMA did not demonstrate a discrepancy in efficacy of PAR2 and PAR1 inhibition.

Teleocidin A2 confirms preference for PAR2 blockade in PAR2$^{-/-}$ murine PASMC

To assess Ca^{2+} mobilization in murine pulmonary smooth muscle cells (WT and PAR2$^{-/-}$), cells were stimulated with
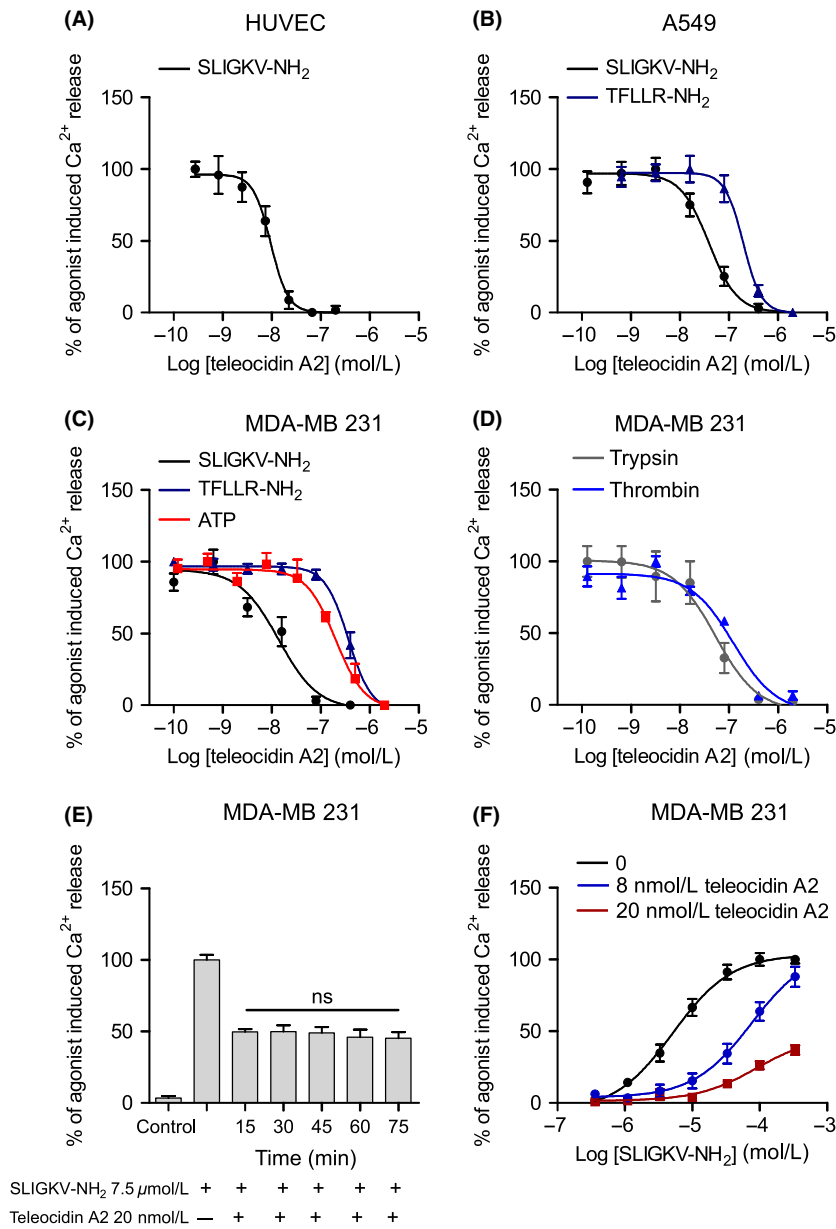
Figure 3. Inhibition of intracellular Ca^{2+} mobilization by teleocidin A2 in HUVEC, A549, and MDA-MB 231 cells. (A) Concentration-dependent curves of PAR2 (SLIGKV-NH$_2$) inhibition by teleocidin A2 in HUVEC. (B) Concentration-dependent curves of PAR2 (SLIGKV-NH$_2$) and PAR1 (TFLLR-NH$_2$) receptor inhibition by teleocidin A2 in A549 cells. (C, D) Concentration-dependent curves of PAR2 (SLIGKV-NH$_2$ and trypsin), PAR1 (TFLLR-NH$_2$ and thrombin), and P2Y (ATP) receptor inhibition by teleocidin A2 in MDA-MB 231 cells. Results represent means $\pm$ SEM, $n \geq 3$ (*n*, number of replicates). (E) Time dependency of teleocidin A2 induced PAR2-mediated Ca^{2+} release inhibition. Data shown in bar charts are means $\pm$ SEM from three independent experiments performed in triplicates, ns, not statistically significant. (F) Concentration-dependent activity curves of teleocidin A2 versus varying concentrations of PAR2 agonist SLIGKV-NH$_2$. HUVEC, human umbilical vein endothelial cell; A549, lung carcinoma cell line; MDA-MB 231, human breast adenocarcinoma cell line; PAR2, proteinase-activated receptor 2.

the PAR2 agonists murine peptide SLIGRL-NH$_2$ and trypsin or the PAR1 agonists TFLLR-NH$_2$ and thrombin. A markedly reduced stimulation of intracellular Ca^{2+} release by SLIGRL-NH$_2$ or trypsin in mPASMC PAR2$^{-/-}$ in comparison to WT was noted. As expected, no difference in PAR1 agonist peptide-mediated Ca^{2+} mobilization in

PAR2$^{-/-}$ compared to WT was seen. However, in contrast to the tethered PAR1 ligand for thrombin, a significantly reduced signal could be detected in mPASMC PAR2$^{-/-}$ (Fig. 5A), which is consistent with the reported findings for thrombin in MDA-MB 231 cells (Fig. 3D). As thrombin significantly differentiated between PAR2$^{-/-}$ and WT cells,
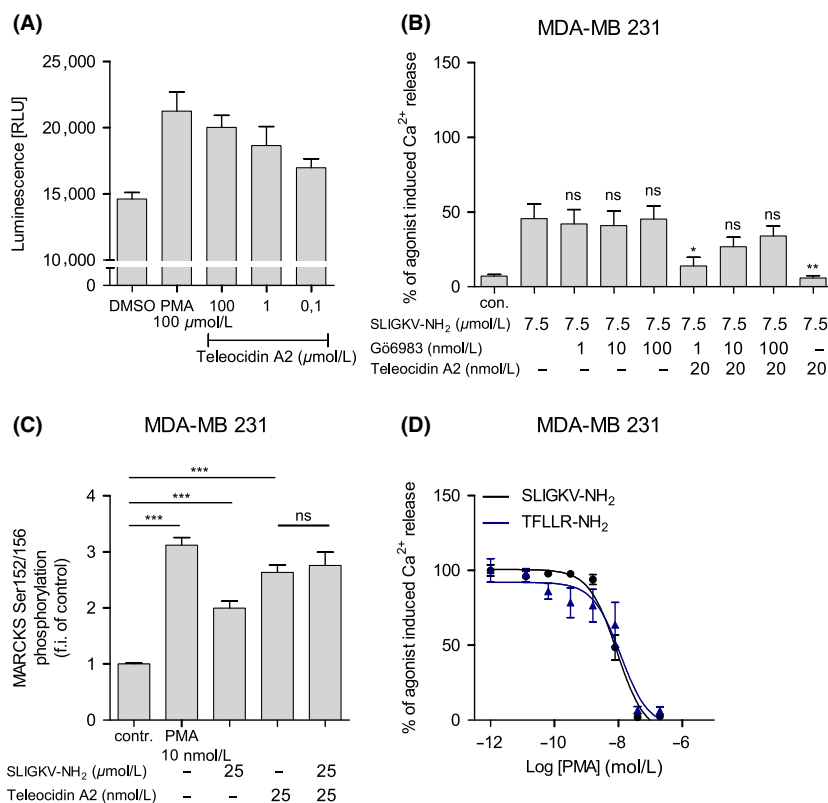
Figure 4. (A) Biochemical PKC ADP-Glo kinase assay. Teleocidin A2 activates purified PKC mix containing isoforms α, β, and γ in high micromolar ranges in the presence of phosphatidylserine, but in the absence of diacylglycerol and calcium. Generated ADP during kinase reaction was measured using ADP-Glo™ kinase assay. (B) PKC inhibitor Gö6983 reverses teleocidin A2-mediated inhibition of PAR2-induced Ca^{2+} release in MDA-MB 231 cells. Inhibition of PKC with 1, 10, and 100 nmol/L Gö6983 has no impact on PAR2-induced intracellular Ca^{2+} release. However, the inhibitory effect of 20 nmol/L teleocidin A2 on PAR2 Ca^{2+} release is reversed with increasing Gö6983 concentrations. Gö6983 was preincubated before teleocidin A2 addition and activation of PAR2 with SLIGKV-NH$_2$. (C) PKC activation as detected by phospho-MARCKS (Ser152/156) ELISA; f.i., fold increase. Data shown in bar chart are means ± SEM from three independent experiments performed in triplicates; ns, not statistically significant; *$P < 0.05$, **$P < 0.01$, ***$P < 0.001$. (D) Inhibition of intracellular Ca^{2+} mobilization by PKC activator PMA. Results represent means ± SEM, $n \geq 3$ (n, number of replicates). PKC, protein kinase C; PAR2, proteinase-activated receptor 2; MDA-MB 231, human breast adenocarcinoma cell line; PMA, phorbol 12-myristate 13-acetate.

subsequent studies to assess the effects of teleocidin A2 in mPASMC were performed using the PAR1 agonist peptide TFLLR-NH$_2$ with comparably EC$_{50}$ values in both WT and PAR2$^{-/-}$ cells. Determined IC$_{50}$ values (IC$_{50}$ 24.6 ± 4.2 nmol/L and 862 ± 214 nmol/L for mPASMC WT and PAR2$^{-/-}$, respectively) confirmed that in the presence of PAR2, telocidin is significantly more efficacious in inhibiting Ca^{2+} mobilization. Thus, the reported preference of teleocidin A2 for PAR2 blockade in human tumor cell lines (Fig. 5B, Table 1) could be verified in murine PAR2$^{-/-}$ cells.

Teleocidin A2 does not displace SLIGKV-NH$_2$ binding to PAR2

Based on the striking efficacious PAR2 antagonistic effect, it was obvious to further address whether teleocidin A2

acts mechanistically via direct competition with SLIGKV-NH$_2$ or with the formed N-terminal sequence upon protease cleavage. Thus, binding of teleocidin A2 to human PAR2 in recombinant Hela cells was evaluated in competition with radiolabeled [3H]2-f-LIGRL-NH$_2$. Inhibition of control-specific binding by 0.5 and 5 μmol/L teleocidin A2 was below 4%, and thus considered to be nonsignificant (Table 2). In conclusion, teleocidin A2 does not compete with the binding of radiolabeled [3H]2-f-LIGRL-NH$_2$ PAR2.

Teleocidin A2 antagonizes cell migration

PAR2 has been associated with increased cellular motility in various cancer cell types. Migration of MDA-MB 231 in the presence and absence of teleocidin A2 and various stimuli was examined in a cell migratory exclusion assay
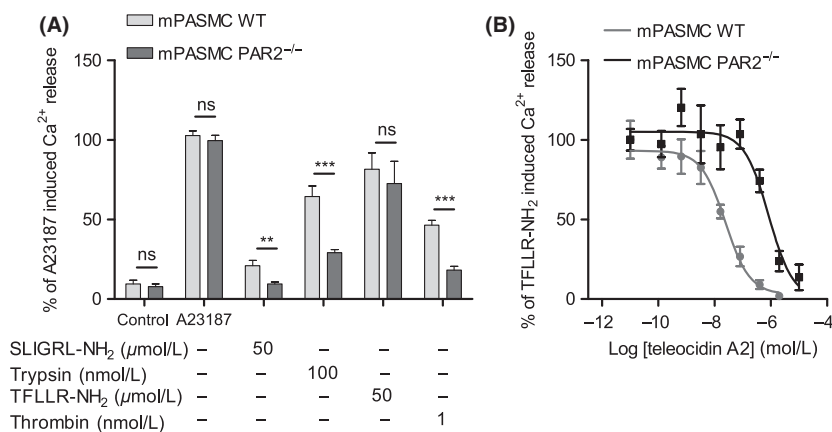
Figure 5. (A) Intracellular Ca^{2+} mobilization in mPASMC. (A) PAR2 (SLIGRL-NH$_2$ and trypsin) and PAR1 (TFLLR-NH$_2$ and thrombin) agonist stimulated release of intracellular Ca^{2+} in mPASMC WT and mPASMC PAR2$^{-/-}$. Maximum fluorescence was detected by 10 μmol/L of the ionophore A23187. Data shown in bar charts are means $\pm$ SEM from three independent experiments performed in triplicates; ns, not statistically significant; **$P < 0.01$, ***$P < 0.001$. (B) Inhibition of intracellular Ca^{2+} mobilization by teleocidin A2. Concentration-dependent curves of PAR1 inhibition by teleocidin A2 in mPASMC WT and mPASMC PAR2$^{-/-}$. Results represent data (mean $\pm$ SEM) of four independent experiments performed in triplicates. mPASMC, murine pulmonary artery smooth muscle cells; PAR, proteinase-activated receptor; WT, wild type.

Table 2. Radioligand binding assay.

Compound	Test concentration	% Inhibition of control specific binding
Teleocidin A2	0.5 μmol/L	-2.05 ± 9.82
	5 μmol/L	3.75 ± 3.18

IC$_{50}$ value of reference compound SLIGRL-NH$_2$ for inhibition of control specific binding was 0.12 μmol/L. Inhibition levels of control specific (labeled PAR2 peptide) binding higher than 50% indicate at significant binding of test compounds. PAR2, proteinase-activated receptor 2.

to explore the effect upon PAR2-stimulated chemokinesis. Trypsin (5 nmol/L) and SLIGKV-NH$_2$ (25 μmol/L) significantly enhanced the migration of MDA-MB 231 by twofold to basal values after 48 h (Fig. 6A and B). To examine whether teleocidin A2 suppresses PAR2-induced cell migration, cells were preincubated with 25 nmol/L compound and then stimulated with either 25 μmol/L SLIGKV-NH$_2$ or 5 nmol/L trypsin. Teleocidin A2 reduced SLIGKV-NH$_2$- and trypsin-stimulated migration to the level of basal values. When incubated alone, the compound had no effect upon basal cellular motility (Fig. 6B). To confirm the effect demonstrated in cell migration to be solely based on increased cellular motility, a cell viability assay was conducted in parallel at the same experimental conditions. No significant change in cell viability occurred upon PAR2 stimulation (with either trypsin or SLIGKV-NH$_2$) or after inhibition via teleocidin A2, respectively (Fig. 6C). Moreover, the reported data show enhanced cell proliferation upon PAR2 stimulation

by neither trypsin or SLIGKV-NH$_2$ nor teleocidin A2 alone.

Rac1 controls PAR2-mediated migration

PAR2-induced signaling cascade leading to cell migration in MDA-MB 231 cells was further examined by applying various inhibitors of PAR2 downstream effector proteins. PKC antagonist Gö6983 (Gschwendt et al. 1996) was incubated along with 25 μmol/L SLIGKV-NH$_2$. However, PKC inhibition failed to significantly block PAR2-induced cell migration (Fig. 7A). On the other hand, PKC inhibitor Gö6983, applied at 100 nmol/L, distinctly reduced the level of PAR2-induced phosphorylation of the specific endogenous PKC substrate MARCKS in MDA-MB 231 cells (Fig. 7B), suggesting that the PAR2–Ca^{2+}–PKC signaling axis is not involved in PAR2-induced migration in the selected cell line.

Rho-associated coiled-coil forming protein kinase (ROCK) family inhibitor Y27632 (Ishizaki et al. 2000) potentiated the SLIGKV-NH$_2$-induced migration by twofold in comparison to SLIGKV-NH$_2$ and by fourfold in comparison to the basal migration, whereas the inhibitor alone had no significant effect on MDA-MB 231 basal cell migration (Fig. 7C). Small GTPase Rac1 inhibitor EHop-016 (Montalvo-Ortiz et al. 2012) (2 μmol/L) was incubated along with SLIGKV-NH$_2$ in the cell migratory exclusion assay (Fig. 7D). EHop-016 reduced SLIGKV-NH$_2$ (25 μmol/L)-stimulated migration to 100% basal migration, and therefore completely blocked the SLIGKV-NH$_2$-induced effect. Furthermore, the stimulatory effect
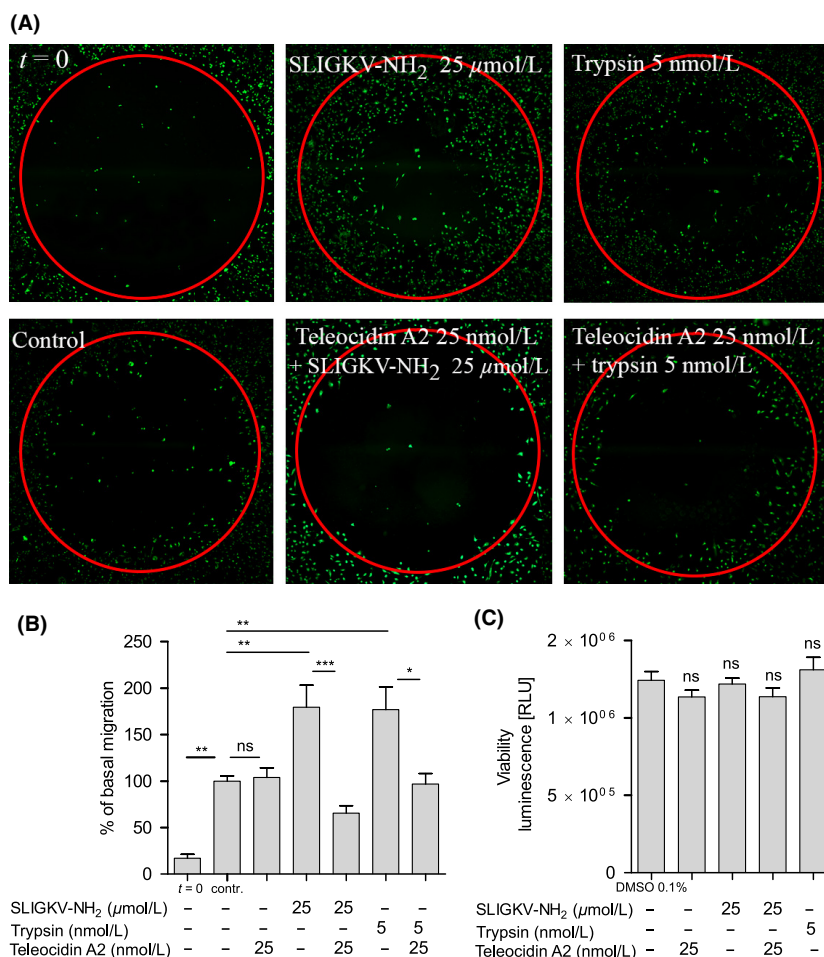
(A)

(B)

(C)

Figure 6. Teleocidin A2 interferes with PAR2-mediated cell migration. (A) Teleocidin A2 reverses SLIGKV-NH$_2$ or trypsin induced migration in a cell exclusion assay. Microscopy images show representative data of migration into detection zone after 48 h from three independent experiments. Cell culture medium was used as negative control. (B) Cell migration into detection zone shown in (A) was analyzed by particle analysis in ImageJ and basal migration after 48 h (control) was set to 100%. (C) Cell viability of MDA-MB 231 is influenced neither by teleocidin A2 nor by SLIGKV-NH$_2$ or trypsin. MDA-MB 231 cells were treated at the same conditions as in the migration assay and the amount of viable cells was detected using CellTiter-Glo® assay reagent. After a treatment period of 48 h, testing conditions had no statistically significant impact on cell viability when compared to DMSO control. Data shown in bar charts are mean values from three independent experiments with $n \geq 3$ (n, number of replicates); ns, not statistically significant; *$P < 0.05$, **$P < 0.01$, ***$P < 0.001$. PAR, proteinase-activated receptor; MDA-MB 231, human breast adenocarcinoma cell line.

of trypsin (5 nmol/L) on MDA-MB 231 cell migration was significantly reduced to 100% basal migration in the presence of EHop-016, confirming the significant role of Rac1 in PAR2-induced cell migration. Ehop-016 alone, however, had no influence on basal tumor cell migration (Fig. 7D).

Influence of PAR2 and teleocidin A2 on actin cytoskeleton rearrangement

The migration of cells is based on a dynamic actin cytoskeleton undergoing constant and directed rearrangement. PAR2

activation has been associated with both increased migratory capacities and rearrangement of actin cytoskeleton. To further determine the role of PAR2 and the influence of teleocidin A2 on actin cytoskeletal rearrangement, MDA-MB 231 cells were treated with PAR2 agonist SLIGKV-NH$_2$ in the presence and absence of teleocidin A2 or inhibitors of putative PAR2 downstream effectors. SLIGKV-NH$_2$ induced reorganization of the actin cytoskeleton and markedly increased the number of stress fibers (Fig. 8). Preincubation of the cells with either 1 μmol/L ROCK1/2 inhibitor Y27632 or 2 μmol/L Rac1 inhibitor EHop-016 followed by stimulation with SLIGKV-NH$_2$ initiated distinct reorganization of
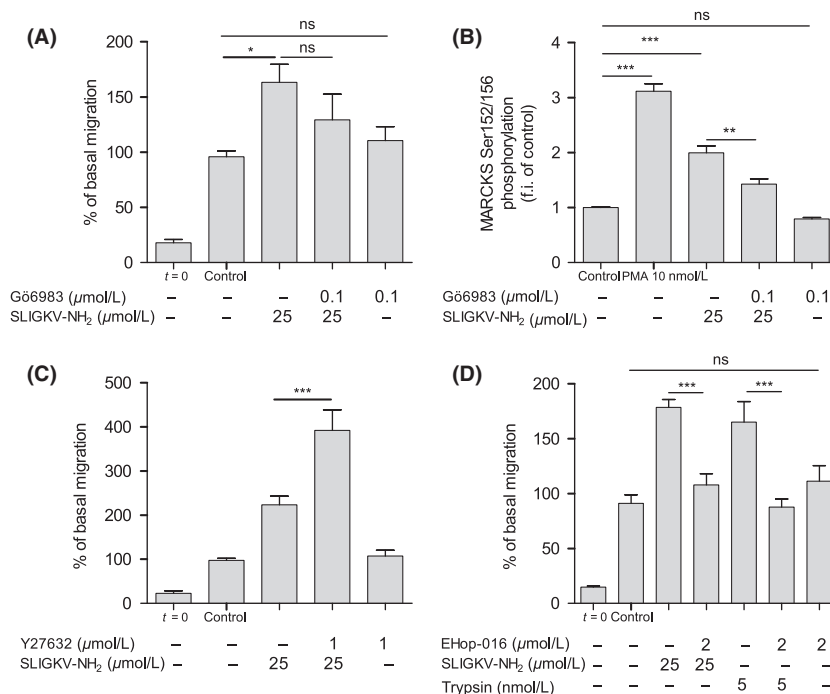
Figure 7. Effects of pan PKC inhibitor Gö6983, Rac1 inhibitor EHop-016, and ROCK1/2 inhibitor Y27632 on PAR2-mediated cell migration. (A) PKC inhibition does not significantly block PAR2-induced cell migration. (B) SLIGKV-NH$_2$ induced intracellular PKC activation and inhibition by 100 nmol/L Gö6983 detected by phospho-MARCKS (Ser152/156) ELISA, f.i. fold increase. (C) Y27632 potentiates SLIGKV-NH$_2$-mediated cell migration. (D) SLIGKV-NH$_2$ – PAR2-mediated cell migration is regulated via Rac1. Cell migration into detection zone was analyzed by particle analysis in ImageJ and basal migration after 48 h (control) was set to 100%. Data shown in bar chart are means ± SEM from three independent experiments with $n \geq 3$ (n, number of replicates); ns, not statistically significant; *$P < 0.05$, **$P < 0.01$, ***$P < 0.001$. PKC, protein kinase C; Rac1, ras-related C3 botulinum toxin substrate 1; ROCK1/2, Rho-associated, coiled-coil containing protein kinase 1/2; PAR, proteinase-activated receptor; MARCKS, myristolated alanine-rich protein kinase C substrate.

the actin cytoskeleton. Actin cytoskeletal organization of cells pretreated with Rac1 inhibitor EHop-016 was markedly changed in the majority of observed cells, supporting the prominent role of Rac1 in PAR2-mediated tumor cell migration. The inhibition of ROCK1/2 which is a downstream target of small GTPase RhoA led to a less frequent alteration of cell morphology, but reduced the number of visible stress fibers in comparison to PAR2 AP-treated control cells (Fig. 8).

With respect to the anti-PAR2 migratory effect of teleocidin A2 in the cell migration assay, the compound was examined for its potential to inhibit PAR2-induced actin rearrangement. PAR2-induced stress fiber formation was suppressed by 20 nmol/L teleocidin A2, however, teleocidin A2 treatment led to the development of distinct actin fiber accumulation at the cell membrane and membrane ruffles (Fig. 8). Although this effect was also observed after treatment with teleocidin A2 alone, suggesting a second, presumably PAR2-independent role of the compound in regulating cytoskeleton rearrangement, teleocidin A2 did not alter basal cellular motility of MDA-MB 231.

Discussion and Conclusions

Due to their importance in the control of many pathophysiological processes, GPCRs are the primary targets for over 30% of clinically used drugs (reviewed in Jacoby et al. 2006; Zhao et al. 2014). Most PAR-related drug discovery research to date has focused on PAR1. PAR1 receptor antagonist vorapaxar (SCH 530348, Merck) gained FDA approval in 2014 for antiplatelet therapy and is the first marketed antagonist of the PAR family (Chackalamannil et al. 2008). However, the development of effective PAR2 antagonists remains in the early stages.

The distinct role of PAR2 in multiple pathophysiological contexts strongly illustrates the need for PAR2 inhibitors to further investigate PAR2 biology. All PAR2 antagonists described to date, however, are limited in potency and selectivity, combined with a deficiency to completely antagonize PAR2 signaling. For example, the small molecule antagonist ENMD-1068 achieved in vitro potency only in the low millimolar concentration range (Kelso et al. 2006). The peptide mimetic antagonist K14585 failed to inhibit protease-dependent PAR2 signaling (Goh
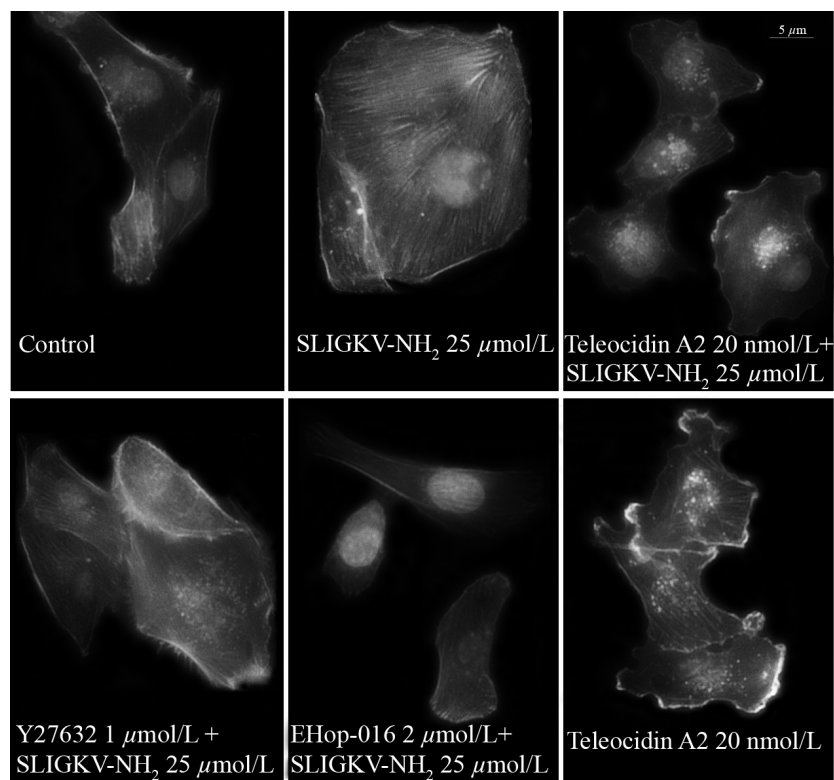
Figure 8. Actin cytoskeleton rearrangement. Fluorescent microscopy images of Alexa Fluor 546-conjugated phalloidin and DAPI-stained MDA-MB 231 cells. SLIGKV-NH$_2$ – proteinase-activated receptor 2 activation causes stress fiber formation. Cells were treated with either SLIGKV-NH$_2$ (25 μmol/L, 30 min) or teleocidin A2 alone (20 nmol/L, 30 min) or teleocidin A2 (20 nmol/L), Y27632 (1 μmol/L), and EHop-016 (2 μmol/L) in the presence of SLIGKV-NH$_2$ (25 μmol/L). MDA-MB 231, human breast adenocarcinoma cell line.

et al. 2009; Kanke et al. 2009). The PAR2 antagonist GB88 achieved antagonistic activity at low micromolar concentrations in vitro and demonstrated efficacy in vivo. However, subsequent studies revealed biased agonist or antagonist activity (Barry et al. 2010; Lohman et al. 2012; Suen et al. 2014). The most recently published antagonist C391 was able to inhibit PAR2-dependent Ca^{2+} release and mitogen-activated protein kinase (MAPK) signals (IC$_{50}$ 1.3 μmol/L), but showed partial agonistic activity already at concentrations of 10 μmol/L (Boitano et al. 2015).

In this study, we confirm the natural product teleocidin A2 as a potent inhibitor of PAR2 signaling. For the first time, our data reveal that teleocidin A2 inhibits PAR2-dependent intracellular Ca^{2+} mobilization with remarkable efficacy (IC$_{50}$ values between 15 and 25 nmol/L) in MDA-MB 231 breast cancer, A549 lung carcinoma, and HUVEC. The high potency of teleocidin A2 was observed for both structurally divergent activating PAR2 agonists, the peptide tethered ligand-derived agonist SLIGKV-NH$_2$, as well as the endogenous activating protease trypsin. In contrast to MDA-MB 231 cells, noncancerous primary breast epithelial cells (HMEC) showed only insignificant

Ca^{2+} mobilization upon PAR2 stimulation. These data are consistent with previous findings (Su et al. 2009) which demonstrated upregulated PAR2 protein level in cancerous breast tissue in comparison to healthy normal breast tissues, supporting PAR2 as an attractive cancer target. In contrast to the PAR2 agonists described earlier, teleocidin A2 itself, however, did not induce significant agonistic effects on intracellular Ca^{2+} mobilization up to concentrations of 1 μmol/L. Furthermore, the amount of teleocidin A2-induced Ca^{2+} inhibition remained stable for at least 75 min.

To date, teleocidin derivatives are mainly categorized as tumor-promoting agents. Although studies suggest that activation of PKC might play a major role in the mechanism of teleocidin-induced tumor promotion, the decisive PKC-activating concentration of teleocidins is still unclear and mainly based on biochemical data. In radioactive kinase assays, PKC was activated by either 100 nmol/L of an undefined teleocidin (Arcoleo and Weinstein 1985) or by 1–10 μmol/L of teleocidin A2 (Imamoto et al. 1993). Indolactam V, representing a teleocidin scaffold, was shown to activate the PKC substrate MARCKS in a cell-based assay at 200 nmol/L (Meseguer et al. 2000).

Based on the reported significant variations in PKC activating potency, a biochemical PKC kinase assay has been established. Our assay data reveal that teleocidin A2 is able to activate a PKC isoform mixture (primarily α, β, and γ and lesser amounts of δ and ζ isoforms) at high micromolar concentrations, which is consistent with the reported findings from Imamoto et al. (1993). Thus, in comparison to the demonstrated remarkable IC_{50} values in the PAR2 Ca^{2+} mobilization assay, a significant potency loss for teleocidin A2-induced PKC activation in the biochemical kinase assay was noted. In contrast, in the established cellular readout monitoring PKC-dependent phosphorylation of MARCKs teleocidin was able to induce significant phosphorylation at a much lower concentration (25 nmol/L teleocidin), results of which are consistent with previously reported findings (Meseguer et al. 2000).

Moreover, in additional studies to evaluate compound specificity, teleocidin A2 inhibited Ca^{2+} mobilization induced by PAR1 or P2Y with a significant potency loss in comparison to PAR2 inhibition, respectively. In contrast, the PKC activator phorbol ester tumor promoter PMA inhibited both PAR2- and PAR1-mediated Ca^{2+} releases, similarly in the low nanomolar range. Thus, in contrast to the described pronounced PAR2 blocking effect for teleocidin, PMA did not demonstrate a preference for PAR2 inhibition. Former studies showed PMA to be able to reduce bradykinin-induced Ca^{2+} release, indicating that PMA might act through activation of PKC (Luo et al. 1995). Consistent with a hypothesis of a general PKC-mediated effect, Ca^{2+} mobilization of the G_q-coupled GPCRs PAR1 and P2Y are influenced by

teleocidin A2. However, the PMA data clearly reveal that a solely PKC-mediated effect cannot explain the remarkable efficacy of teleocidin A2 on PAR2-mediated signaling. The cell-based kinase assay results are consistent with our findings that teleocidin-mediated blockade of PAR2 Ca^{2+} release was suppressed in the presence of a PKC inhibitor, although PAR2-induced Ca^{2+} release alone was not influenced by PKC inhibition. Despite the undisputable role of teleocidin as a potent PKC activator, it remains elusive how the ability to activate PKC mechanistically acts on PAR2-induced Ca^{2+} mobilization (Fig. 9).

Although increasing concentrations of teleocidin A2 reduced the maximum response of SLIGKV-NH$_2$-induced intracellular Ca^{2+} mobilization, in a radioligand binding assay, teleocidin A2 did not displace binding of the labeled PAR2 agonist peptide [^{3}H]2-furoyl-LIGRL-NH$_2$, presumably hinting at an unknown modulation site of teleocidin A2 to mediate its inhibitory potency. Identification of the modulation site of teleocidin A2 is in the focus of our current research activities.

Importantly, the reported results from murine pulmonary smooth muscle cells (WT and PAR2$^{-/-}$) confirmed that in the presence of PAR2, teleocidin is significantly more efficacious in inhibiting Ca^{2+} mobilization. However, studies in the PAR2$^{-/-}$ cells further revealed a putative unspecificity for thrombin as a PAR1 agonist, indicating that the generated tethered ligand of PAR$_1$ by thrombin can bind and activate PAR2, resulting in intermolecular signaling as described previously (Ossovskaya and Bunnett 2004). Moreover, a heterodimerization of PAR2 and PAR1 to form a functional signaling unit cannot be ruled out (Jaber et al.
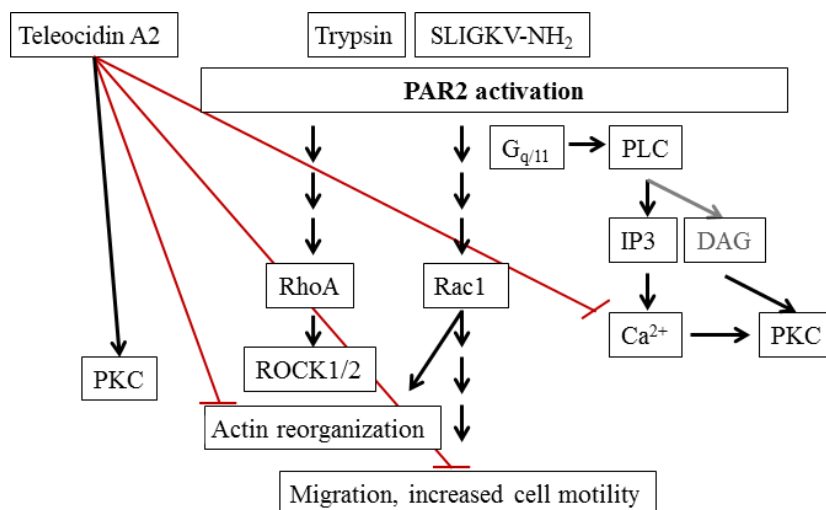

Figure 9. Hypothesis of teleocidin A2-regulated blockade of PAR2 signaling pathways. Teleocidin A2 was able to potently inhibit PAR2-induced intracellular Ca^{2+} mobilization and antagonized PAR2-dependent cellular motility, presumably interfering with cancer cell migration by reorganization of the actin cytoskeleton. PAR2, proteinase-activated receptor 2; PLC, phospholipase C; IP3, inositol 1,4,5-trisphosphate; DAG, diacylglycerol; PKC, protein kinase C; ROCK1/2, rho-associated, coiled-coil containing protein kinase 1/2.

2014) and would require further experiments including knockout studies.

Our data show that stimulation by SLIGKV-NH$_2$ and trypsin significantly increased the number of migrated MDA-MB 231 cells, confirming the described role of PAR2 in promoting cell migration. Teleocidin A2 reduced PAR2-induced migration to the basal control level. The compound itself had no effect on cellular motility. In conclusion, additionally to the inhibition of intracellular G$_q$-coupled Ca^{2+} mobilization, teleocidin A2 is able to inhibit PAR2-induced cell motility at low nanomolar concentrations. Furthermore, teleocidin A2 does not enhance proliferation or migration of breast cancer cells and is not cytotoxic during the investigated incubation time.

As cell migration is based on a dynamic actin cytoskeleton rearrangement, the role of PAR2 and the distinct influence of teleocidin A2 on actin cytoskeletal rearrangement have been explored. The impact of PKC in PAR2 signaling contributing to cell migration is likely cell-type dependent (Ahamed and Ruf 2004; Wu et al. 2013). Our investigations suggest that PAR2 PKC inhibition failed to significantly block PAR2-induced cell migration, again indicating that teleocidin is able to induce cellular signaling independent of PKC. In contrast, the small GTPase Rac1 reveals to be one of the key regulators in promoting dynamic actin reorganization crucial for breast cancer cell migration. Small GTPases are well characterized to act on actin dynamics being important regulators for the balanced assembly and disassembly of actin bundles and focal adhesions (Raftopoulou and Hall 2004). Both RhoA and Rac1 were described to be involved in the PAR2 signaling cascade, either in case of RhoA leading to the formation of stress fibers and focal adhesions (Greenberg et al. 2003; Sriwai et al. 2013) or in case of Rac1 controlling cell migration via a c-src–Rac1–JNK 1/2 signaling pathway (Su et al. 2009). Rac1 inhibitor EHop-016 inhibited PAR2-induced cell migration which is consistent with the findings of Su et al. (2009). Additionally, Rac1 inhibition blocked the PAR2 induced, uniquely defined actin bundles. Thus, upon Rac1 inhibition cell morphology resembled the diffuse actin staining of control cells.

ROCK is one downstream target activated by RhoA that was shown to be a key player in stress fiber formation and in focal adhesion organization (Ishizaki et al. 2000). Interestingly, inhibition of RhoA downstream target ROCK1/2 enhanced PAR2-induced migration, but not proliferation of MDA-MB 231 cells. RhoA and Rac1 were described to mediate opposing activities in cell migration. Moreover, a strong activation of RhoA can even be inhibitory to cell migration in certain cell types (McHardy et al. 2004; Brew et al. 2009). Our data confirm distinct stress fiber formation upon PAR2 stimulation.

Furthermore, aggressive breast cancer cell line MDA-MB 231 has been characterized by constitutive activation and overexpression of RhoA (Pillé et al. 2005). Together, this may lead to significantly increased ROCK1/2 activation in MDA-MB 231 cells accompanied by rigid and less flexible network of actin bundles limiting cell migration, while ROCK1/2 inhibition results in enhanced cell migration.

Finally, the impact of teleocidin A2 on PAR2 characteristic actin rearrangement has been investigated. Teleocidin A2 abolished PAR2-dependent cytoskeletal effects. Thus, we propose that the inhibitory function of teleocidin A2 on PAR2-induced cell migration is dependent on reorganization of actin cytoskeleton. Teleocidin A2 led to prominent lamellipodia formation and actin enrichment at the cell membrane. These findings are consistent with results from Deng et al. (2010) who observed an increase in cell spreading upon stimulation with a teleocidin mixture in fibroblasts proposing an underlying signaling cascade involving PKD and Rac1 activation.

In summary, this study reveals teleocidin A2 as a potent inhibitor of PAR2-induced signaling cascades relevant for tumor progression in cancer cells (Fig. 9). Teleocidin A2 is able to inhibit Ca^{2+} mobilization induced by PAR2-specific agonists. Interestingly, in contrast to PAR1 or P2Y, PAR2-dependent signaling is inhibited by teleocidin A2 with remarkable potency, suggesting a preference of teleocidin for PAR2 blockade. Although we cannot rule out an involvement of PKC in the mechanism of action of teleocidin A2 to date, based on our knowledge from GPCR Ca^{2+} and PMA inhibition data, the blocking effect on PAR2 signaling might not be exclusively dependent on activation of PKC. Furthermore, teleocidin A2 inhibits PAR2-induced cellular motility at low nanomolar concentrations presumably independent from PKC activation. Moreover, teleocidin A2 might control cancer cell migration by modulating PAR2-induced actin cytoskeletal reorganization.

To further explore the divergent biological functions of teleocidin A2 independent from PKC in a cellular context, we intent to validate functional receptor knockout studies. Additionally, screening of a teleocidin library might hint at a structure activity relationship regarding PAR2 inhibition. Thus, a medicinal chemistry approach has been started to design novel derivatives depicting high efficacy in PAR2 antagonism, but no activation of cellular PKC to provide the basis for the development of a novel therapeutic anti-cancer strategy.

Acknowledgements

WT and PAR2$^{-/-}$ were a kind gift from Rosenkranz (University Hospital Cologne).

Disclosures

References

Ahamed J, Ruf W (2004). Protease-activated receptor 2-dependent phosphorylation of the tissue factor cytoplasmic domain. J Biol Chem 279: 23038–23044.

Arcoleo JP, Weinstein IB (1985). Activation of protein kinase C by tumor promoting phorbol esters, teleocidin and aplysiatoxin in the absence of added calcium. Carcinogenesis 6: 213–217.

Bao Y, Hou W, Hua B (2014). Protease-activated receptor 2 signalling pathways: a role in pain processing. Expert Opin Ther Targets 18: 15–27.

Barry GD, Suen JY, Le GT, Cotterell A, Reid RC, Fairlie DP (2010). Novel agonists and antagonists for human protease activated receptor 2. J Med Chem 53: 7428–7440.

Boitano S, Hoffman J, Flynn AN, Asiedu MN, Tillu DV, Zhang Z, et al. (2015). The novel PAR2 ligand C391 blocks multiple PAR2 signalling pathways in vitro and in vivo. Br J Pharmacol 172: 4535–4545.

Brew CT, Aronchik I, Kosco K, McCammon J, Bjeldanes LF, Firestone GL (2009). Indole-3-carbinol inhibits MDA-MB-231 breast cancer cell motility and induces stress fibers and focal adhesion formation by activation of Rho kinase activity. Int J Cancer 124: 2294–2302.

Chackalamannil S, Wang Y, Greenlee WJ, Hu Z, Xia Y, Ahn H, et al. (2008). Discovery of a novel, orally active himbacine-based thrombin receptor antagonist (SCH 530348) with potent antiplatelet activity. J Med Chem 51: 3061–3064.

D'Andrea MR, Derian CK, Santulli RJ, Andrade-Gordon P (2001). Differential expression of protease-activated receptors-1 and -2 in stromal fibroblasts of normal, benign, and malignant human tissues. Am J Pathol 158: 2031–2041.

DeFea KA, Zalevsky J, Thoma MS, Déry O, Mullins RD, Bunnett NW (2000). beta-Arrestin-dependent endocytosis of proteinase-activated receptor 2 is required for intracellular targeting of activated ERK1/2. J Cell Biol 148: 1267–1281.

Deng K, Gao Y, Cao Z, Graziani EI, Wood A, Doherty P, et al. (2010). Overcoming amino-Nogo-induced inhibition of cell spreading and neurite outgrowth by 12-O-tetradecanoylphorbol-13-acetate-type tumor promoters. J Biol Chem 285: 6425–6433.

Elste AP, Petersen I (2010). Expression of proteinase-activated receptor 1-4 (PAR 1-4) in human cancer. J Mol Histol 41: 89–99.

ten Freyhaus H, Berghausen EM, Janssen W, Leuchs M, Zierden M, Murmann K, et al. (2015). Genetic ablation of PDGF-dependent signaling pathways abolishes vascular remodeling and experimental pulmonary hypertension. Arterioscler Thromb Vasc Biol 35: 1236–1245.

Fujiki H, Tanaka Y, Miyake R, Kikkawa U, Nishizuka Y, Sugimura T (1984). Activation of calcium-activated, phospholipid-dependent protein kinase (protein kinase C) by new classes of tumor promoters: teleocidin and debromoaplysiatoxin. Biochem Biophys Res Commun 120: 339–343.

Gieseler F, Ungefroren H, Settmacher U, Hollenberg MD, Kaufmann R (2013). Proteinase-activated receptors (PARs) – focus on receptor-receptor-interactions and their physiological and pathophysiological impact. Cell Commun Signal 11: 86.

Goh FG, Ng PY, Nilsson M, Kanke T, Plevin R (2009). Dual effect of the novel peptide antagonist K-14585 on proteinase-activated receptor-2-mediated signalling. Br J Pharmacol 158: 1695–1704.

Gough W, Hulkower KI, Lynch R, McGlynn P, Uhlik M, Yan L, et al. (2011). A quantitative, facile, and high-throughput image-based cell migration method is a robust alternative to the scratch assay. J Biomol Screen 16: 155–163.

Greenberg DL, Mize GJ, Takayama TK (2003). Protease-activated receptor mediated RhoA signaling and cytoskeletal reorganization in LNCaP cells. Biochemistry 42: 702–709.

Gschwendt M, Dieterich S, Rennecke J, Kittstein W, Mueller HJ, Johannes FJ (1996). Inhibition of protein kinase C mu by various inhibitors. Differentiation from protein kinase c isoenzymes. FEBS Lett 392: 77–80.

Heemskerk FM, Chen HC, Huang FL (1993). Protein kinase C phosphorylates Ser152, Ser156 and Ser163 but not Ser160 of MARCKS in rat brain. Biochem Biophys Res Commun 190: 236–241.

Hjortoe GM, Petersen LC, Albrektsen T, Sorensen BB, Norby PL, Mandal SK, et al. (2004). Tissue factor-factor VIIa-specific up-regulation of IL-8 expression in MDA-MB-231 cells is mediated by PAR-2 and results in increased cell migration. Blood 103: 3029–3037.

Hu L, Xia L, Zhou H, Wu B, Mu Y, Wu Y, et al. (2013). TF/FVIIa/PAR2 promotes cell proliferation and migration via PKCα and ERK-dependent c-Jun/AP-1 pathway in colon cancer cell line SW620. Tumour Biol 34: 2573–2581.

Huang S, Li Y, Chen H, Rong J, Ye S (2013). Activation of proteinase-activated receptor 2 prevents apoptosis of lung cancer cells. Cancer Invest 31: 578–581.

Imamoto A, Wang XJ, Fujiki H, Walker SE, Beltran LM, DiGiovanni J (1993). Comparison of 12-O-tetradecanoylphorbol-13-acetate and teleocidin for induction of epidermal hyperplasia, activation of epidermal PKC

isozymes and skin tumor promotion in SENCAR and C57BL/6 mice. Carcinogenesis 14: 719–724.

Ishihara H, Connolly AJ, Zeng D, Kahn ML, Zheng YW, Timmons C, et al. (1997). Protease-activated receptor 3 is a second thrombin receptor in humans. Nature 386: 502–506.

Ishizaki T, Uehata M, Tamechika I, Keel J, Nonomura K, Maekawa M, et al. (2000). Pharmacological properties of Y-27632, a specific inhibitor of rho-associated kinases. Mol Pharmacol 57: 976–983.

Jaber M, Maoz M, Kancharla A, Agranovich D, Perez T, Grisaru-Granovsky S, et al. (2014). Prorease-activated-receptor-2 affects protease-activated-receptor-1 driven breast cancer. Cell Mol Life Sci 71: 2517–2533.

Jacoby E, Bouhelal R, Gerspacher M, Seuwen K (2006). The 7 TM G-protein-coupled receptor target family. ChemMedChem 1: 761–782.

Kanke T, Ishiwata H, Kabeya M, Saka M, Doi T, Hattori Y, et al. (2005). Binding of a highly potent protease-activated receptor-2 (PAR2) activating peptide, [3H]2-furoyl-LIGRL-NH2, to human PAR2. Br J Pharmacol 145:255–263.

Kanke T, Kabeya M, Kubo S, Kondo S, Yasuoka K, Tagashira J, et al. (2009). Novel antagonists for proteinase-activated receptor 2: inhibition of cellular and vascular responses in vitro and in vivo. Br J Pharmacol 158: 361–371.

Kaufmann R, Mussbach F, Henklein P, Settmacher U (2011). Proteinase-activated receptor 2-mediated calcium signaling in hepatocellular carcinoma cells. J Cancer Res Clin Oncol 137: 965–973.

Kelso EB, Lockhart JC, Hembrough T, Dunning L, Plevin R, Hollenberg MD, et al. (2006). Therapeutic promise of proteinase-activated receptor-2 antagonism in joint inflammation. J Pharmacol Exp Ther 316: 1017–1024.

Li S, Jiang P, Xiang Y, Wang W, Zhu Y, Feng W, et al. (2014). Protease-activated receptor (PAR)1, PAR2 and PAR4 expressions in esophageal squamous cell carcinoma. Dongwuxue Yanjiu 35: 420–425.

Lohman R, Cotterell AJ, Barry GD, Liu L, Suen JY, Vesey DA, et al. (2012). An antagonist of human protease activated receptor-2 attenuates PAR2 signaling, macrophage activation, mast cell degranulation, and collagen-induced arthritis in rats. FASEB J 26: 2877–2887.

Luo S, Tsao H, Ong R, Hsiehz J, Yang CM (1995). Inhibitory effect of phorbol ester on bradykinin-induced phosphoinositide hydrolysis and calcium mobilization in cultured canine tracheal smooth muscle cells. Cell Signal 7: 571–581.

McHardy LM, Sinotte R, Troussard A, Sheldon C, Church J, Williams DE, et al. (2004). The tumor invasion inhibitor dihydromotuporamine C activates RHO, remodels stress fibers and focal adhesions, and stimulates sodium-proton exchange. Cancer Res 64: 1468–1474.

Meseguer B, Alonso-Díaz D, Griebenow N, Herget T, Waldmann H (2000). Solid-phase synthesis and biological evaluation of a teleocidin library–discovery of a selective PKCdelta down regulator. Chemistry 6: 3943–3957.

Montalvo-Ortiz BL, Castillo-Pichardo L, Hernández E, Humphries-Bickley T, De la Mota-Peynado A, Cubano LA, et al. (2012). Characterization of EHop-016, novel small molecule inhibitor of Rac GTPase. J Biol Chem 287: 13228–13238.

Nakanuma S, Tajima H, Okamoto K, Hayashi H, Nakagawara H, Onishi I, et al. (2010). Tumor-derived trypsin enhances proliferation of intrahepatic cholangiocarcinoma cells by activating protease-activated receptor-2. Int J Oncol 36: 793–800.

Nystedt S, Emilsson K, Wahlestedt C, Sundelin J (1994). Molecular cloning of a potential proteinase activated receptor. Proc Natl Acad Sci USA 91: 9208–9212.

Ossovskaya VS, Bunnett NW (2004). Protease-activated receptors: contribution to physiology and disease. Physiol Rev 84: 579–621.

Pillé J, Denoyelle C, Varet J, Bertrand J, Soria J, Opolon P, et al. (2005). Anti-RhoA and anti-RhoC siRNAs inhibit the proliferation and invasiveness of MDA-MB-231 breast cancer cells in vitro and in vivo. Mol Ther 11: 267–274.

Raftopoulou M, Hall A (2004). Cell migration: Rho GTPases lead the way. Dev Biol 265: 23–32.

Rothmeier AS, Ruf W (2012). Protease-activated receptor 2 signaling in inflammation. Semin Immunopathol 34: 133–149.

Rydén L, Grabau D, Schaffner F, Jönsson P, Ruf W, Belting M (2010). Evidence for tissue factor phosphorylation and its correlation with protease-activated receptor expression and the prognosis of primary breast cancer. Int J Cancer 126: 2330–2340.

Scarborough RM, Naughton MA, Teng W, Hung DT, Rose J, Vu TK, et al. (1992). Tethered ligand agonist peptides. Structural requirements for thrombin receptor activation reveal mechanism of proteolytic unmasking of agonist function. J Biol Chem 267: 13146–13149.

Shi K, Queiroz KCS, Stap J, Richel DJ, Spek CA (2013). Protease-activated receptor-2 induces migration of pancreatic cancer cells in an extracellular ATP-dependent manner. J Thromb Haemost 11: 1892–1902.

Sriwai W, Mahavadi S, Al-Shboul O, Grider JR, Murthy KS (2013). Distinctive G protein-dependent signaling by protease-activated receptor 2 (PAR2) in smooth muscle: feedback inhibition of RhoA by cAMP-independent PKA. PLoS One 8: e66743.

Su S, Li Y, Luo Y, Sheng Y, Su Y, Padia RN, et al. (2009). Proteinase-activated receptor 2 expression in breast cancer and its role in breast cancer cell migration. Oncogene 28: 3047–3057.

Suen JY, Barry GD, Lohman RJ, Halili MA, Cotterell AJ, Le GT, et al. (2012). Modulating human proteinase activated

receptor 2 with a novel antagonist (GB88) and agonist (GB110). Br J Pharmacol 165: 1413–1423.

Suen JY, Cotterell A, Lohman RJ, Lim J, Han A, Yau MK, et al. (2014). Pathway-selective antagonism of proteinase activated receptor 2. Br J Pharmacol 171: 4112–4124.

Svensson KJ, Kucharzewska P, Christianson HC, Sköld S, Löfstedt T, Johansson MC, et al. (2011). Hypoxia triggers a proangiogenic pathway involving cancer cell microvesicles and PAR-2-mediated heparin-binding EGF signaling in endothelial cells. Proc Natl Acad Sci USA 108: 13147–13152.

Versteeg HH, Schaffner F, Kerver M, Ellies LG, Andrade-Gordon P, Mueller BM, et al. (2008). Protease-activated receptor (PAR) 2, but not PAR1, signaling promotes the development of mammary adenocarcinoma in polyoma middle T mice. Cancer Res 68: 7219–7227.

Vu TK, Hung DT, Wheaton VI, Coughlin SR (1991). Molecular cloning of a functional thrombin receptor reveals a novel proteolytic mechanism of receptor activation. Cell 64: 1057–1068.

Wu B, Zhou H, Hu L, Mu Y, Wu Y (2013). Involvement of PKCα activation in TF/VIIa/PAR2-induced proliferation, migration, and survival of colon cancer cell SW620. Tumour Biol 34: 837–846.

Xie L, Duan Z, Liu C, Zheng Y, Zhou J (2015). Protease-activated receptor 2 agonist increases cell proliferation and invasion of human pancreatic cancer cells. Exp Ther Med 9: 239–244.

Xu WF, Andersen H, Whitmore TE, Presnell SR, Yee DP, Ching A, et al. (1998). Cloning and characterization of human protease-activated receptor 4. Proc Natl Acad Sci USA 95: 6642–6646.

Zhao P, Metcalf M, Bunnett NW (2014). Biased signaling of protease-activated receptors. Front Endocrinol (Lausanne) 5: 67.

Zhu T, Mancini JA, Sapieha P, Yang C, Joyal J, Honoré J, et al. (2011). Cortactin activation by FVIIa/tissue factor and PAR2 promotes endothelial cell migration. Am J Physiol Regul Integr Comp Physiol 300: R577–R585.

Zoudilova M, Min J, Richards HL, Carter D, Huang T, DeFea KA (2010). beta-Arrestins scaffold cofilin with chronophin to direct localized actin filament severing and membrane protrusions downstream of protease-activated receptor-2. J Biol Chem 285: 14318–14329.

Supporting Information

Additional Supporting Information may be found online in the supporting information tab for this article:

Table S1. *PAR2* gene expression analysis in MDA-MB 231 and HMEC cells. Total RNA was isolated from cells and transcribed (1 μg) to cDNA. The cDNA content was determined by qPCR amplification using gene-specific primers. *PAR2* expression was normalized to the housekeeping genes *GAPDH* and *HPRT1*. The data represent ΔCq mean $\pm$ SEM from three independent experiments performed in triplicates with ΔCq = Cq (PAR2) − Cq (housekeeping gene).

Figure S1. Cell viability. PAR2-mediated cell migration and its inhibition by EHop-016 as shown in Figure 7 is not mediated by proliferative or toxic effects, respectively. MDA-MB 231 cells were treated at the same conditions as described in the migration assay. Amount of viable cells was detected using CellTiter-Glo® assay reagent. (A) Testing conditions had no statistically significant impact on cell viability compared to DMSO control after a treatment period of 48 h as determined with one-way ANOVA and Dunnett's post hoc test relative to the respective mean value of 0.1% DMSO. (B) Single inhibitor controls had no statistically significant impact on cell viability as determined with one-way ANOVA and Dunnett's post hoc test relative to the respective mean value of 0.1% DMSO. All data represent mean value $\pm$ SEM of five independent experiments performed in triplicate; ns, not statistically significant; *$P < 0.05$, **$P < 0.01$, ***$P < 0.001$.

Figure S2. Stimulation of MDA-MB 231 cells with PAR4 AP AYPGKF-NH2. Kinetics of intracellular Ca^{2+} release in MDA-MB 231 upon stimulation with 10 μmol/L SLIGKV-NH2, 5 nmol/L trypsin, or 10 μmol/L/30 μmol/L AYPGKF-NH2. Maximum fluorescence was detected by 10 μmol/L of the ionophore A23187. Results represent data from at least three independent experiments performed in triplicates.

Figure S3. Inhibition of trypsin- and thrombin-induced Ca^{2+} release in MDA-MB 231 by vorapaxar. (A, B) Vorapaxar inhibited thrombin-induced PAR1 Ca^{2+} signaling in a dose-dependent manner, but not trypsin-induced PAR2-dependent Ca^{2+} signaling. Data shown in bar charts are mean values from three independent experiments with $n \geq 3$ (n, number of replicates); ns, not statistically significant; *$P < 0.05$, **$P < 0.01$, ***$P < 0.001$.